PHYSICAL REVIEW B **81**, 081305(R) (2010)

Excitonic interactions with intense terahertz pulses in ZnSe/ZnMgSSe multiple quantum wells

Hideki Hirori,[1,2,*] Masaya Nagai,[3] and Koichiro Tanaka[1,2,3]
[1]*Institute for Integrated Cell-Material Sciences, Kyoto University, Sakyo-ku, Kyoto 606-8501, Japan*
[2]*CREST, Japan Science and Technology Agency, Kawaguchi, Saitama 332-0012, Japan*
[3]*Department of Physics, Graduate School of Science, Kyoto University, Sakyo-ku, Kyoto 606-8502, Japan*
(Received 22 December 2009; published 23 February 2010)

We studied the interaction of excitons with terahertz (THz) electric fields in ZnSe/ZnMgSSe multiple quantum wells with THz-pump and optical-probe spectroscopy. The incident THz pulse with a peak electric field of ~70 kV/cm induces strong spectral modulations in the heavy-hole and light-hole excitonic absorption resonances. The dependence of the excitonic absorption resonance energy on the THz field follows the Stark effect for smaller THz fields. For larger THz fields, the peak shift deviates from the Stark effect, which implies that the interaction enters the nonperturbative regime.

DOI: 10.1103/PhysRevB.81.081305 PACS number(s): 78.66.Hf, 42.50.Hz, 42.65.Ky, 71.35.−y

The nonlinear interaction of matter with strong oscillating electric fields has attracted considerable attention from researchers because of its importance in fundamental physics and for technological applications such as electro-optic devices. The resonant (or nearly resonant) interaction of electric fields with electronic transitions in semiconductors and atomic gases exhibits intriguing nonlinear phenomena such as the ac (optical) Stark effect,[1,2] Rabi oscillations,[3] Autler-Townes splitting,[1,4] and electromagnetically induced transparency.[5] Even in nonresonant situations, atomic systems subjected to high-intensity laser excitation exhibit extreme nonlinear phenomena such as above-threshold ionization[6] and high-order harmonic generation,[7] and these phenomena cannot be described by perturbation theory. The key concept required to understand these nonperturbative phenomena is ponderomotive energy, which is the cycle-averaged kinetic energy of a wiggling electron in an oscillating electric field.[8]

The recent development of terahertz (THz) pulse technologies has made possible the study in the time domain of the interaction of hydrogenlike excitons in semiconductors with strong THz electric fields.[9–13] For a given laser intensity, the ponderomotive energy of the THz electric field can be $\sim 10^4$ times larger than that of a visible-light source because of the small photon energy of THz radiation.[14] The effects of such interactions may also be enhanced due to the smaller effective mass of carriers in semiconductors relative to the free-electron mass.[14–16] Moreover, exotic many-body effects in quantum-confined systems make semiconductors even richer than single atoms.[17] In particular, excitons in II-VI semiconductors have a relatively large binding energy compared to those in III-V semiconductors,[10,15,16,18] which allows us to study II-VI excitonic interactions using nonresonant THz-field excitation. Furthermore, such studies would complement the studies on atomic nonperturbative phenomena.

In this Rapid Communication, we report the interaction of excitons in ZnSe/ZnMgSSe multiple quantum wells (MQWs) with THz electric fields studied using THz-pump and optical-probe spectroscopy. The THz photon energy is lesser than the exciton binding energy and is small enough to treat the excitation as nonresonant. The incident THz pulse with a maximum electric field of 68 kV/cm induces strong spectral modulations in the excitonic resonances. The THz-field dependence and the temporal response of the excitonic absorption provide clear evidence of the Stark effect with a subpicosecond response time. The deviation observed in the peak shift of the excitonic absorption from what was expected in the Stark effect implies that, for larger THz fields, the interaction enters the nonperturbative regime.

Figure 1(a) shows a schematic of the THz-pump and optical-probe experiment. To generate intense THz pulses, we tilted the pulse-intensity front using a grating-lens combination to match the noncollinear velocity in the $LiNbO_3$ crystal.[19–21] The light source was an amplified Ti:sapphire laser (repetition rate 1 kHz, central wavelength 780 nm, pulse duration 150 fs). Figure 1(b) shows the observed THz temporal profile [measured via THz electro-optic (EO) sampling with a 300-μm-thick GaP detection crystal] and its Fourier components. The THz-pulse beam focus was set to a

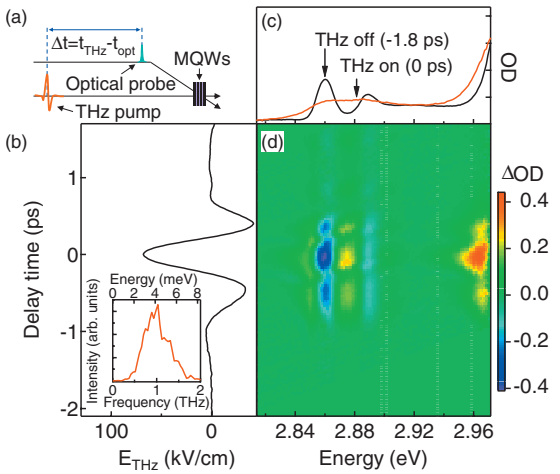

FIG. 1. (Color) (a) Schematic of THz-pump and optical-probe experimental setup. The linear polarization directions of both the pump and probe pulse are the same and parallel to the MQW layers. (b) Observed THz temporal profile and its Fourier components. (c) Excitonic absorption spectra observed at pump-probe delay times of −1.8 (THz pump off) and 0 ps (THz pump on). (d) Differential absorption spectrum of the sample because of the THz pulse, shown as a function of optical energy and delay time between THz-pump and optical-probe pulses.

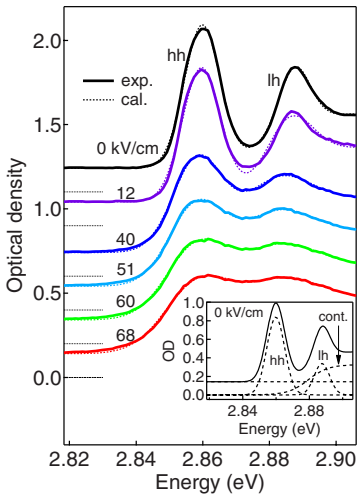

FIG. 2. (Color online) Absorption spectra in the vicinity of the hh and lh excitonic resonances obtained at a delay time of 0 ps for different incident THz fields E_{THz}. Solid and dashed lines correspond to the experimental data and calculated fits, respectively. Inset shows the calculated result of 0 kV/cm (solid line), which is decomposed into the sum of two Gaussian excitons, a broadened 2D continuum, and a background (dashed lines).

diameter of 1.5 mm in the sample using a 90° off-axis parabolic mirror with a focal length of 100 mm. The maximum THz field at the sample position was estimated to be 68 kV/cm by calibrating the EO sampling signal.[22] For the probe pulse, we used a white-light continuum generated by focusing a small portion of the pulsed laser beam into a 10-mm-thick quartz cell containing water. The generated continuum spectrum ranged from the visible to near infrared. The probe beam was focused to a spot on the sample of ~150 μm diameter.

After passing through the sample, the probe pulse was spectrally resolved with a spectrometer (with a resolution of ~2 meV) and detected using a Si linear image sensor. To obtain a high S/N ratio, we synchronously chopped the pump beam for THz generation at 500 Hz, thereby blocking every other pump pulse. A computer collected the signals and divided them to obtain the probe transmission with and without the influence of the THz pump. The MQW sample was grown on a (100) GaAs substrate with a 300 nm GaAs epilayer by the molecular-beam epitaxy technique, followed by 20 nm ZnSe and 1 μm ZnMgSSe buffer layers. The MQWs consist of 30 repetitions of 5 nm ZnSe wells and 30 nm ZnMgSSe barriers. For optical-absorption measurements, the substrate was removed by wet etching. All experiments were done at temperatures below 6 K.

Figure 1(d) presents the differential absorption spectrum of the sample induced by the incident THz pulse as a function of optical energy and delay time between the THz-pump and optical-probe pulses. Figure 1(c) shows the optical-absorption spectrum with the THz pump off and THz pump on (i.e., at pump-probe delay times of −1.8 and 0 ps, respectively). Here, the large chirp present in the broadband probe over the time range considered (~1 ps) obliges us to account for the chirp in processing the data but does not affect the interpretation of the effect. The absorption peaks at 2.86 and 2.89 eV in the pump-off spectra in Fig. 1(c) are due to $n=1$ heavy-hole (hh) and light-hole (lh) excitonic absorptions, respectively. The energy splitting between the hh and lh excitons is caused by the stress imposed on the well layers that remove the valence-band degeneracy at $k=0$. In the presence of the THz pump, the absorption increases below the band edge of the ZnMgSSe (bulk barrier layer) and in the region above 2.92 eV. This behavior is attributed to the dynamical Frantz-Keldysh effect (DFKE).[14–16]

Figure 2 shows the absorption spectra in the vicinity of the hh and lh excitonic absorption resonances obtained at the delay time of 0 ps. A pair of wire-grid polarizers was used to attenuate the THz pulses (without modifying the wave form) for the intensity-dependence studies. With increasing THz electric field, the hh and lh excitonic absorption resonances are broadened and redshifted. To evaluate these behaviors quantitatively, we fit the data to[23]

$$\alpha(\omega) = \alpha_{\mathrm{hh}} \exp\left(-\frac{(\hbar\omega - \hbar\Omega_{\mathrm{hh}})^2}{2(\Gamma_{\mathrm{hh}})^2}\right) + \alpha_{\mathrm{lh}} \exp\left(\frac{(\hbar\omega - \hbar\Omega_{\mathrm{lh}})^2}{2(\Gamma_{\mathrm{lh}})^2}\right) + \frac{\alpha_c}{1+\exp\left(\frac{\hbar\Omega_c - \hbar\omega}{\Gamma_c}\right)} F(\omega) + B, \quad (1)$$

where B is the background contribution, $F(\omega)$ is the Sommerfeld factor,[24] α_i, $\hbar\Omega_i$, and Γ_i (i=hh and lh; c for continuum) are the amplitudes of the corresponding functions, absorption-peak energies, and damping constants, respectively. Here, $2\pi\hbar$ is Planck's constant. Equation (1) is a semiempirical equation that assumes that the absorption spectra consist of two excitons (hh and lh) and the continuum for a two-dimensional (2D) density of states.

Fitting the undistorted experimental spectrum ($E_{\mathrm{THz}}=0$) to Eq. (1) with ten fitting parameters (α_i, Ω_i, Γ_i, and B) and fixed $R_y=18$ meV,[25] we obtain the best-fit curve (dashed line) shown in Fig. 2. The decomposed components are shown in the inset of Fig. 2. An inhomogeneous linewidth broadening because of monolayer fluctuations of the well width, strain, and alloy disorder may dominate the linewidth of excitonic and conduction-band spectra ($\Gamma_{\mathrm{hh,lh},c}=5.4$, 4.6, and 6.0 meV, respectively). The binding energy of the hh exciton ($E_B=19.6$ meV), deduced from the difference between the energies $\hbar\Omega_{\mathrm{hh}}$ and $\hbar\Omega_c$, may become slightly larger than that in the bulk crystal (18 meV) because of the quantum confinement effect on the excitons. Then the THz pulse ($\hbar\omega\sim4$ meV) shown in Fig. 1(b) is far from resonant with the $1s$-$2p$ transition energy of the hh exciton. Figure 2 also shows that Eq. (1) agrees well with the distorted experimental spectra ($E_{\mathrm{THz}}\neq0$). When Eq. (1) is fit to the distorted spectra ($E_{\mathrm{THz}}\neq0$), the parameters describing the continuum band edge (α_c, Ω_c, and Γ_c) and the parameter B deduced from fitting the undistorted spectrum ($E_{\mathrm{THz}}=0$) are used as fixed parameters.[26]

The interaction of the THz field and the exciton causes a distortion of the Coulomb potential between the electron and hole, causing the Coulomb well to widen, which in turn induces a shift in the $1s$ level.[27] Figure 3(a) shows the dependence on the THz field of the hh and lh excitonic peak energies (the data for this figure are derived from the fits shown

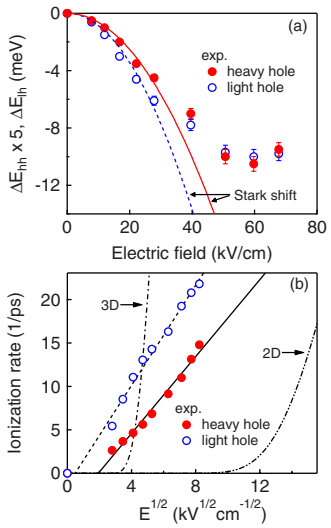

FIG. 3. (Color online) (a) Dependence on the energy of the absorption resonance of the hh (solid circles) and lh (open circles) excitons on the incident THz field E_{THz}, derived from the fits shown in Fig. 2. Solid and dashed lines are fits of Eq. (2) to the data for the hh and lh excitons, respectively. (b) Field-dependent ionization rate $\gamma(E_{\mathrm{THz}})$ of the hh (solid circles) and lh (open circles) excitons. The one-dot-dashed line and two-dot-dashed line show the calculated tunneling ionization rate for the case of 3D and 2D excitons. The solid and dashed lines are guides for the $\sqrt{E_{\mathrm{THz}}}$ dependence.

in Fig. 2). Both excitonic absorption resonances redshift monotonically with increasing THz field until ~60 kV/cm. Upon further increasing the THz field, the redshift trend ceases and even reverses to become a blueshift trend. The usual perturbative theory of the Stark effect may be approximately applicable in the weak-field limit because of a far-resonant condition, giving the following quadratic Stark shifts in the 1*s* exciton state:[28]

$$\delta E_S = -\kappa \frac{(ea_B \tilde{t} E_{\mathrm{THz}})^2}{R_y}, \tag{2}$$

where κ is a fitting parameter, e is the elementary charge, a_B is the bulk Bohr radius (4.5 nm),[25] R_y is the Rydberg energy (18 meV),[25] $\tilde{t}$ is the transmission coefficient,[29] and E_{THz} is the maximum electric-field amplitude of the incident THz pulse.

As shown in Fig. 3(a), fitting Eq. (2) to the data from 0 to 28 kV/cm indicates that the excitonic absorption resonances are well described by the quadratic Stark shift. The best fit to hh exciton data studied here is obtained with $\kappa \sim 0.4$, which is much smaller than the theoretical value for ideal, three-dimensional (3D) 1*s* excitons ($\kappa_{3D}=9/8$) and approaches the 2D case ($\kappa_{2D}=21/512$).[28] The fitting parameter obtained for the lh exciton ($\kappa \sim 3$) is much larger than that for the hh exciton, which may be due to the larger Bohr radius and smaller binding energy of the lh exciton with respect to the hh exciton.

The departure of the experimental data from the quadratic Stark shift occurs at stronger THz fields and the blueshift trend of the excitonic absorption resonance implies a competition of two different nonperturbative phenomena. The first phenomenon is that the high THz field dominates the excitonic Coulomb potential and induces the mixing of excitonic states with continuum states, because for high THz fields, the Keldysh parameter (KP) is sufficiently less than unity. Specifically, $KP=\sqrt{E_B/(2U_P)}=\sqrt{(19.6\ \mathrm{meV})/(2\times 64\ \mathrm{meV})} \sim 0.4$ at $E_{\mathrm{THz}}=60$ kV/cm.[8,30] Additionally, the incident maximum THz field exceeds the static electric field necessary to ionize the hh exciton, which is estimated by $E_B/ea_B \sim 44$ kV/cm. The second phenomenon may be that the DFKE causes a blueshift of the band edge of the 2D electronic continuum states.[15]

The field ionization of a bound excitonic state occurs when the Coulomb-correlated electron-hole pair disassociates because of the THz field, and this ionization results in a reduction in the coherent lifetime of the exciton. As shown in Fig. 2, this process manifests itself as a spectral broadening of the excitonic absorption resonance. The linewidth enhancement because of field-induced ionization can be characterized by a field-dependent linewidth $\Gamma^i(E_{\mathrm{THz}})$. We define the field-induced ionization rate $\gamma(E_{\mathrm{THz}})$ as $\gamma(E_{\mathrm{THz}})=\Gamma^i(E_{\mathrm{THz}})\sqrt{2\ \ln\ 2}/\hbar=[\Gamma(E_{\mathrm{THz}})^2-\Gamma(0)^2]^{1/2}\sqrt{2\ \ln\ 2}/\hbar$, where $\Gamma(E_{\mathrm{THz}})$ and $\Gamma(0)$ are the damping constants obtained experimentally at nonzero field and zero field, respectively.

Figure 3(b) shows the THz-field dependence of the ionization rate $\gamma(E_{\mathrm{THz}})$. The ionization rate increases monotonically with increasing THz field. To understand the field-ionization mechanism, we compare the experimental results with the theoretically calculated excitonic field-ionization rate, assuming direct electron tunneling through the Coulomb barrier whose height is lowered by the THz field [e.g., Eqs. (A6) and (A7) in Ref. 31]. However, this treatment cannot explain the gradual increase in the experimental data as shown in Fig. 3(b). Conversely, the experimental ionization rate is proportional to a square root of the THz field $\sqrt{E_{\mathrm{THz}}}$. Because the model introduced by Frenkel predicts that the ionization probability increases approximately with $\sqrt{E}$,[32] these experimental results imply that the ionization process may be dominated by a field-enhanced thermal-ionization process, where the ionization energy is supplied by the phonon, but the barrier is lowered by the field. The observation of the signature of phonon-assisted ionization may imply a stronger exciton-phonon coupling in polar II-VI compounds.[18]

It is interesting to show the optical temporal response to the THz pulse of excitons in quantum wells because ultrafast optical modulation via ultrafast electroabsorption in excitons is a potential application. Figure 4 compares the temporal profiles of the absorption change in the vicinity of the hh exciton (at 2.86 eV) and the absolute value of the electric field of the THz pulse. The absorption change follows the THz temporal profile rather closely. The theory of dynamic excitonic electroabsorption based on a one-dimensional exciton predicts that the effective response time is just the dephasing time of the exciton and is the reciprocal of the homogeneous broadening.[33] The dephasing time of the sample at zero field is measured to be ~450 fs by femtosecond four-wave mixing,[34] and it could be sufficiently shortened by applying the THz field. Thus, the subpicosecond electroabsorption response time for excitons implied by the data of Fig. 4 is reasonable.

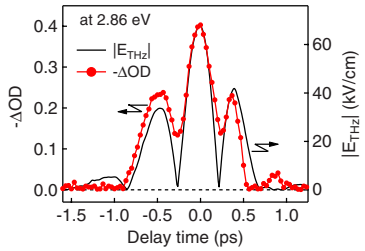

FIG. 4. (Color online) Comparison of the temporal profiles between the absorption change in the vicinity of the hh exciton (at 2.86 eV) and the absolute value of the electric field of the THz pulse.

In conclusion, we studied the interaction of excitons in ZnSe/ZnMgSSe MQWs with THz electric fields. With increasing THz field, the excitonic absorption resonance redshifts and the absorption linewidth broadens. The dependence of the energy of excitonic absorption resonance on the THz field follows perturbation theory (i.e., the Stark shift) for low THz fields, whereas for higher THz fields, the experimental results clearly deviate from this theory. This finding implies that the excitonic interaction with THz field enters the nonperturbative regime. The efficient modulation of the excitonic absorption and the short response time of this absorption in the ZnSe/ZnMgSSe MQWs bode well for applications based on optical modulation via ultrafast excitonic electroabsorption.

We are grateful to Nobuko Naka and Junichiro Kono for valuable discussions. One of the authors (H.H.) was supported by KAKENHI (Grant No. 21760038). This work was also supported by KAKENHI (Grant No. 20104007).

*hirori@icems.kyoto-u.ac.jp

[1] S. H. Autler and C. H. Townes, Phys. Rev. **100**, 703 (1955).
[2] A. Mysyrowicz, D. Hulin, A. Antonetti, A. Migus, W. T. Masselink, and H. Morkoç, Phys. Rev. Lett. **56**, 2748 (1986).
[3] I. I. Rabi, Phys. Rev. **51**, 652 (1937).
[4] S. G. Carter, V. Birkedal, C. S. Wang, L. A. Coldren, A. V. Maslov, D. S. Citrin, and M. S. Sherwin, Science **310**, 651 (2005).
[5] S. E. Harris, J. E. Field, and A. Imamoglu, Phys. Rev. Lett. **64**, 1107 (1990).
[6] P. B. Corkum, N. H. Burnett, and F. Brunel, Phys. Rev. Lett. **62**, 1259 (1989).
[7] M. Y. Ivanov and P. B. Corkum, Phys. Rev. A **48**, 580 (1993).
[8] T. Brabec and F. Krausz, Rev. Mod. Phys. **72**, 545 (2000).
[9] C. W. Luo, K. Reimann, M. Woerner, T. Elsaesser, R. Hey, and K. H. Ploog, Phys. Rev. Lett. **92**, 047402 (2004).
[10] J. R. Danielson, Y.-S. Lee, J. P. Prineas, J. T. Steiner, M. Kira, and S. W. Koch, Phys. Rev. Lett. **99**, 237401 (2007).
[11] S. Leinß, T. Kampfrath, K. v. Volkmann, M. Wolf, J. T. Steiner, M. Kira, S. W. Koch, A. Leitenstorfer, and R. Huber, Phys. Rev. Lett. **101**, 246401 (2008).
[12] L. Razzari, F. H. Su, G. Sharma, F. Blanchard, A. Ayesheshim, H.-C. Bandulet, R. Morandotti, J.-C. Kieffer, T. Ozaki, M. Reid, and F. A. Hegmann, Phys. Rev. B **79**, 193204 (2009).
[13] M. C. Hoffmann, J. Hebling, H. Y. Hwang, K. -L. Yeh, and K. A. Nelson, Phys. Rev. B **79**, 161201(R) (2009).
[14] A. H. Chin, J. M. Bakker, and J. Kono, Phys. Rev. Lett. **85**, 3293 (2000).
[15] K. B. Nordstrom, K. Johnsen, S. J. Allen, A.-P. Jauho, B. Birnir, J. Kono, T. Noda, H. Akiyama, and H. Sakaki, Phys. Rev. Lett. **81**, 457 (1998).
[16] A. Srivastava, R. Srivastava, J. Wang, and J. Kono, Phys. Rev. Lett. **93**, 157401 (2004).
[17] T. Ogawa, in *Optical Properties of Low-Dimensional Materials*, edited by T. Ogawa and Y. Kanemitsu (World Scientific, Singapore, 1995).
[18] C. F. Klingshirm, *Semiconductor Optics* (Springer, Berlin, 1997).
[19] J. Hebling, G. Almási, and J. Kuhl, Opt. Express **10**, 1161 (2002).
[20] J. Hebling, A. G. Stepanov, G. Almási, B. Bartal, and J. Kuhl, Appl. Phys. B: Lasers Opt. **78**, 593 (2004).
[21] M. Jewariya, M. Nagai, and K. Tanaka, J. Opt. Soc. Am. B **26**, A101 (2009).
[22] An EO signal $\Delta I/I$ measured by balanced photodetectors is calibrated to electric-field amplitude E_{THz} (Ref. 21). For the GaP detection crystal used here, the refractive index $n_{\mathrm{opt}}=3.2$ [see *Handbook of Optical Constants of Solids*, edited by E. D. Palik (Academic Press, London, 1985)]; the EO coefficient $r_{41}=1$ pm/V [see Q. Wu and X.-C. Zhang, Appl. Phys. Lett. **70**, 1784 (1997)] and the thickness $L=300$ μm.
[23] D. S. Chemla, D. A. B. Miller, P. W. Smith, A. C. Gossard, and W. Wiegmann, IEEE J. Quantum Electron. **20**, 265 (1984).
[24] The Sommerfield factor in the case of two-dimensional density of states is described by $F(\hbar\omega)=2/\{1+\exp[-2\pi(|\hbar\Omega_C-\hbar\omega|/R_y)^{-1/2}]\}$ (see Ref. 23).
[25] H. E. Gumlich, D. Theis, and D. Tschierse, in *Physics of II-VI and I-VII Compounds*, Landolt-Börnstein, edited by O. Madelung (Springer, Berlin, 1987).
[26] The other fixed parameters, which are α_c and $\hbar\Omega_c$ of the continuum and B of the background contribution, are 0.16, 2.879 eV, and 0.14, respectively. Upon increasing E_{THz} from 0 to 68 kV/cm, α_{hh} and α_{lh} decrease from 0.84 to 0.36 and from 0.34 to 0.24, respectively.
[27] D. F. Blossey, Phys. Rev. B **3**, 1382 (1971).
[28] F. L. Lederman and J. D. Dow, Phys. Rev. B **13**, 1633 (1976).
[29] Fresnel transmission coefficient at the boundary between the sample and air is described by $\tilde{t}=2/(\sqrt{\varepsilon_0}+1)$, where $\varepsilon_0=8.8$ is used as a dielectric constant of the sample (Ref. 25).
[30] The ponderomotive energy is defined by $U_P=e(\tilde{t}E^{in}_{\mathrm{THz}})^2/4m^*\omega^2$ (Ref. 15). Here we used the effective mass $m^*=0.16$ m_0 of ZnSe crystal (Ref. 25), and $\omega/2\pi$ of 1 THz.
[31] D. A. B. Miller, D. S. Chemla, T. C. Damen, A. C. Gossard, W. Wiegmann, T. H. Wood, and C. A. Burrus, Phys. Rev. B **32**, 1043 (1985).
[32] J. Frenkel, Phys. Rev. **54**, 647 (1938).
[33] S. Schmitt-Rink, D. S. Chemla, W. H. Knox, and D. A. B. Miller, Opt. Lett. **15**, 60 (1990).
[34] S. Hataoka, A. Itoh, I. Tanahashi, and K. Tanaka, J. Lumin. **87-89**, 853 (2000).